CHAPTER 2..... 

EXPERIMENTAL

2.1 Materials :

All the chemicals used for the synthesis and characterization of the materials were of A.R. grade. Methanol, hexane, *m*-cresol, aniline and its substituted derivatives like *N*-ethyl aniline, *N*-methyl aniline, *o*-anisidine and *o*-toluidine were distilled twice before use. Double distilled water was used as the solvent wherever necessary. Chloroauric acid ($HAuCl_4$), silver nitrate ($AgNO_3$), palladium chloride ($PdCl_2$), ammonium persulphate and ammonia were used as received without any further processing and purification.

2.1.1 Synthesis of transition metal nanoparticles :

Transition metal nanoparticles of metals such as palladium (Pd), gold (Au) and silver (Ag) were prepared by γ-irradiation of aqueous metal salt solutions in presence of various monomers such as aniline, *N*-ethyl aniline, *N*-methyl aniline, *o*-anisidine and *o*-toluidine so as to investigate the appropriate stabilizer that yields fine sized and stable metal nanoparticles. The concentration of metal ion and stabilizer was also varied during the synthesis of nanoparticles. The concentration of aniline ranged from 0.05 to 1.0 M while that of the metal ion was varied from $1x10^{-4}$ to $1x10^{-2}$ M.

Metal (Pd, Au and Ag) nanoparticles were obtained by irradiating a fixed volume of 100 ml containing the respective metal salt (1×10^{-4}M)

and appropriate amount of aniline in methanol-water (1:1) solvent system in a ^{60}Co γ-source (BARC, Trombay) to a total dose of 198 kGy.

2.1.2 The ^{60}Co γ- ray source :

The irradiation of the samples was carried out in a ^{60}Co gamma source with a dose rate of 10 Gy $Min.^{-1}$, supplied by the Bhabha Atomic Research Centre, Trombay, Bombay. The geometry of the ^{60}Co pencils in the source is arranged in such a fashion that it provides a uniform dose throughout the irradiation cavity. Fig. 2.1 illustrates the design of the source. All the samples were kept in air tight glass bottles with ground glass joints for irradiation. The irradiations were done at room temperature.

2.1.3 Measurement of dose :

The dose rate of ^{60}Co source was determined by Fricke dosimetry. The Fricke solution was prepared by dissolving 0.14 g of $FeSO_4.7H_2O$, 0.03 g NaCl and 11.5 cm^3 of concentrated H_2SO_4 in water and the final volume was made to 500 cm^3. Sodium chloride was added to inhibit the oxidation of ferrous ions by organic impurities. About six tubes each containing 10 cm^3 of the Fricke solution were prepared for irradiation for different time intervals. The dose rate was calculated from equivalents of Fe^{3+} formed and the known $G(Fe^{3+})$ value. The dose absorbed has been calculated by using the following expression

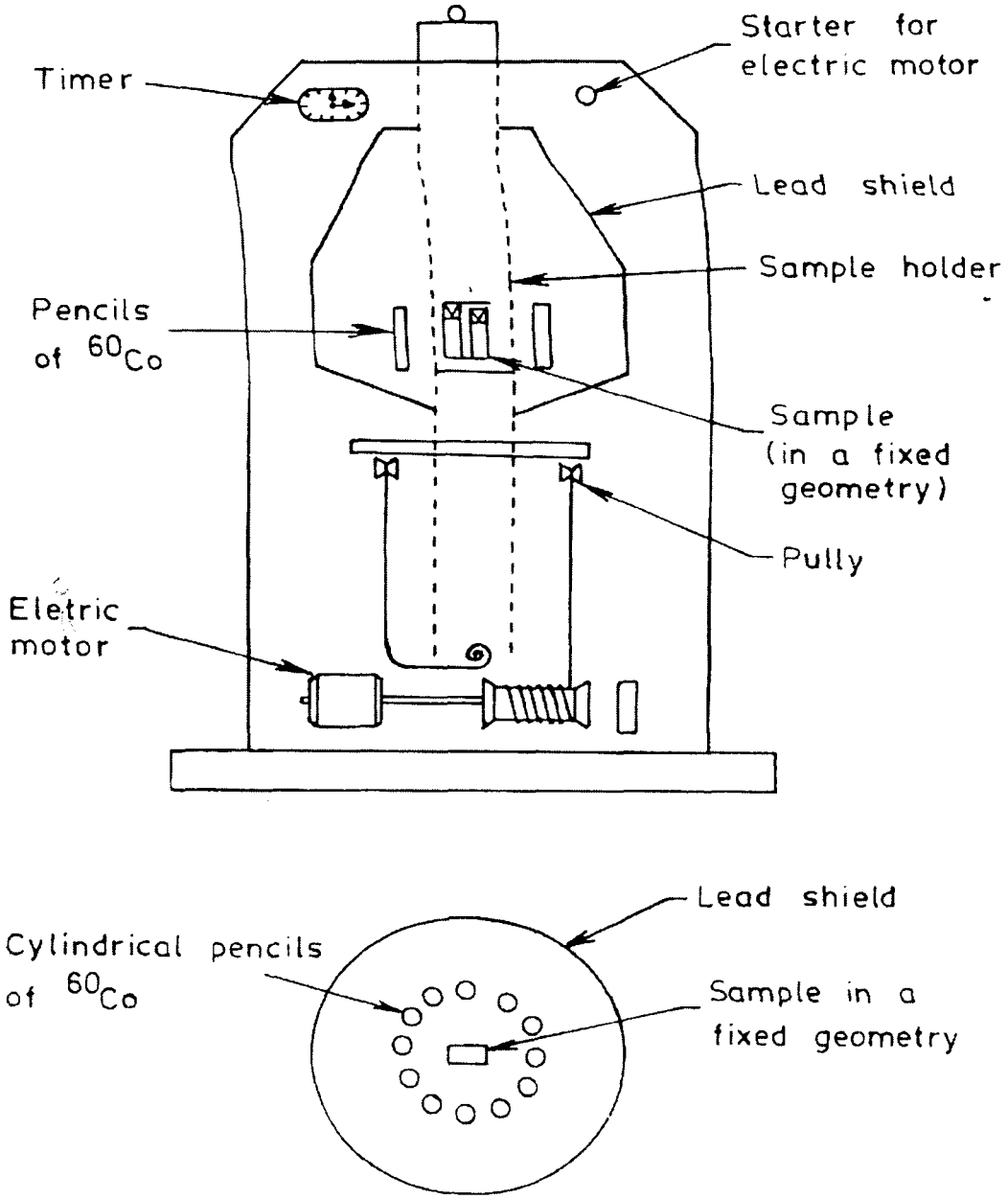

Fig. 2.1 Cross section and top view of the gamma source.

$$\text{Energy absorbed} = \frac{(OD_i - OD_b)\ 0.965 \times 10^9}{\rho\ \varepsilon\ G\ (Fe^{3+}) \times 10^2} \quad Gy$$

Where, OD_i is the optical density of the irradiated dosimeter solution and OD_b is that of non-irradiated solution. ε is the molar extinction coefficient (mol^{-1} cm^2) for ferric ion at the wavelength of maximum absorption (305 nm), d is the thickness (cm) of the cell and ρ is the density (g cm^{-3}) of dosimeter solution. The molar extinction coefficient of Fe^{3+} was determined by measuring the absorbance of various known concentrations of ferric ion at 305 nm wavelength and was found to be 2194 mol^{-1} cm^2 which agrees reasonably with the literature value of 2204 mol^{-1} cm^2. G (Fe^{3+}) was taken as 15.5. The dose rate obtained was measured from time to time.

2.1.4 Decay Scheme of ^{60}Co :

Gamma rays are often produced alongside other forms of radiation such as alpha or beta. When a nucleus emits an α or β particle, the daughter nucleus is sometimes left in an excited state. It can then jump down to a lower level by emitting a gamma ray in the same way as an atomic electron can jump to a lower level by emitting ultraviolet radiation.

Gamma rays, x-rays, visible light, and UV rays are all forms of electromagnetic radiation. The only difference is the frequency and hence the energy of the photons. Gamma rays are the most energetic as compared to others. The Decay Scheme for the ^{60}Co isotope is as follows,

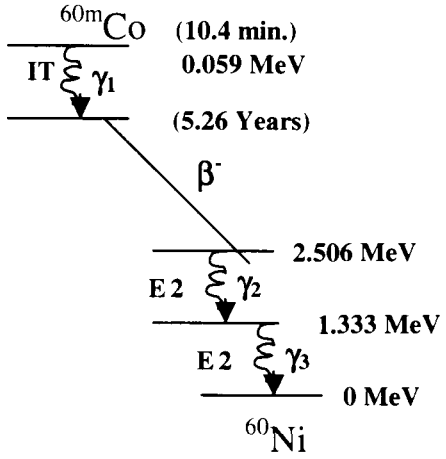

2.2 Synthesis of Metal-Polyaniline Nanocomposites :

Transition metal-polyaniline nanocomposites were synthesized by oxidative polymerization of the metal (Pd, Ag and Au) nanosols containing aniline by drop wise addition of ammonium persulphate to the constantly stirred solution. The temperature was maintained at 5°C for a reaction time of 2 h. The bluish green product thus formed was separated by filtration followed by washing with excess of double distilled water till the pH of filtrate was ~7.0. The product was dried in an oven for 24 h to achieve a constant weight. The yield obtained was ~ 92%.

Similar procedure was repeated in absence of metal salts (Pd, Ag and Au) to synthesize blank polyaniline (Pani) required for comparison.

2.2.1 Reaction mechanism involved in nanoparticle formation :

The γ-radiolysis method utilizes high energy photons of electromagnetic radiations for the synthesis of metal nanoparticles in which water is often used as a solvent.

Water on radiolysis, yields free radicals, ions and molecular products such as

$$H_2O \longrightarrow {}^{\cdot}H + {}^{\cdot}OH + e^-_{aqua} + {}^{\cdot}OH_2 + H_3O^+ + H_2 + H_2O_2 \qquad 2.1$$

Amongst these, the solvated electrons e^-_{aqua} and $^{\cdot}H$ are the strong reducing agents which facilitates the reduction of metal ions to zerovalent metal and hence the nanoparticles.

$$M^+ + e^-_{aqua} \longrightarrow M^0 \qquad 2.2$$

$$M^+ + {}^{\cdot}H \longrightarrow M^0 + H^+ \qquad 2.3$$

On the other hand, $^{\cdot}OH$ radicals being oxidizing in nature would lead to the oxidation of the zerovalent metal [68,69]. Thus, competition arises between the two opposite processes i.e. reduction and oxidation of metal nanoparticles.

As a result, during synthesis of metal nanoparticles by radiation method it is essential to add a reagent in the reaction mixture which will scavenge the $^{\cdot}OH$ radical and avoid the oxidation of metal.

Therefore, in the present case, 1:1 water-methanol solvent system was used as alcohols are well known scavengers for $^{\cdot}OH$ radicals. The

radiolysis of alcohols have been extensively studied by several researchers [70-72].

Methanol on radiolysis undergoes the following reaction,

$$CH_3OH \longrightarrow CH_3O^{\cdot} + {}^{\cdot}H \qquad 2.4$$

This $CH_3O^{\cdot}$ reacts with the ${}^{\cdot}OH$ radicals as -

$$CH_3OH + {}^{\cdot}OH \longrightarrow CHOH + H_2O \qquad 2.5$$

During the nanoparticle formation, aniline also undergoes radiolysis [73] to give the products as –

$$C_6H_5(NH_2) \longrightarrow C_6H_5(NH)^{\cdot} + H^{\cdot} \qquad 2.6$$

The abstracted $H^{\cdot}$ assists the reduction of metal ion while the, two $C_6H_5(NH)^{\cdot}$ radicals react to form a dimer which in turn stabilizes the metal nanoparticles formed by radiolysis.

$$C_6H_5(NH)^{\cdot} + C_6H_5(NH)^{\cdot} \longrightarrow C_6H_5(NH_2)\,C_6H_5 \qquad 2.7$$

2.3 Structural Characterization of Metal Nanoparticles, Polyaniline and Nanocomposites :

The synthesized products were characterized using various analytical techniques. Blank polyaniline was used as reference wherever necessary.

2.3.1 UV-Visible spectroscopy :

Principle

UV-Visible spectroscopy (UV = 200-400 nm, Visible =400-800 nm) corresponds to the electronic excitations between different energy levels of the molecular orbitals of the systems. In particular, transitions

involving π orbitals and lone pairs are important and hence UV-Vis spectroscopy is useful for identifying conjugated systems which tend to have stronger absorbance.

UV-Visible spectroscopy has been used to characterize the metal nanoparticles and metal - polymer nanocomposites as well as polyaniline. Significant changes can be observed in the optical absorption maxima i.e. the plasmon absorption peak with change in the size of the nanoparticles. The optical properties are known to play a key role in the elucidation of the oxidation state of polyaniline. Similarly, in case of polyaniline, λ_{max} changes are observed depending on the oxidation state of the polymer.

The UV-Visible spectra of the synthesized samples were recorded on Perkin – Elmer Lambda 20 and Shimadzu UV-VIS 1600 double beam spectrophotometers. The range of measurement was selected between 200 to 900 nm with a slit width of 2 nm. The metal nanoparticle sols were directly used for recording the UV-Visible spectra against methanol: water mixture or water as reference while for blank polyaniline and nanocomposites, 1 mg of the sample powder was dissolved in NMP or in *m*-cresol using respective solvent as reference.

2.3.2 FT-IR spectroscopy :

Principle

FT-IR spectroscopy bases its functionality on the principle that almost all molecules absorb infra-red light. Molecules with differences of charges in the electronic fields of their atoms produce dipolar moment. This dipolar moment allows infra red photons to interact with the molecule causing excitation to higher vibrational states.

FT-IR spectroscopy is a qualitative technique that provides information related to the structure of the polymer. Chemical structures of the nanocomposites and the changes that occured when the nanocomposites were exposed to various vapours were identified using FT-IR spectroscopy. Based on the changes in the position or intensities of the bands, the mechanism of the sensing behaviour of the nanocomposite towards various vapours or gases has been predicted.

Solid samples of nanocomposites and blank Pani were used for recording the FT-IR spectra. The nanocomposite samples were ground with spectroscopic grade KBr powder and made into a pellet using a stainless steel die having a diameter of 13 mm. Pressure of 7 tons was applied with the help of a hydraulic pump. The ratio of KBr to nanocomposite samples was maintained to be 100:1. The IR spectra of

the samples were recorded from 400 to 4000 cm^{-1} wavenumbers on FT-IR Spectrophotometers (Perkin Elmer 600 and Shimadzu 1750).

2.3.3 X-ray diffraction analysis (XRD) :

Principle

XRD is an another important technique like UV-Visible spectroscopy for characterizing the nanomaterials. The analysis provides key information about the crystallinity, chemical as well as crystal structure of the samples. The d values that appear in the diffractogram are characteristic of the element or compound which enables the identification of the samples. Crystal structure calculations can also be done with the help of d values and one can predict the crystal structure perfectly. Further, the intensity and width of the peak in XRD is largely governed by the size of the particle. Thus, a broad peak with less intensity means the particle size lies in nano regime. Therefore, using Scherrer's equation, particle size can be roughly calculated from the full width at half maxima (FWHM) values of the peak.

Solid nanomaterial samples were made into a pellet form for XRD analysis. A Philips 1710 X-ray diffractometer was used with a copper target providing radiations of 1.540 Å wavelength. The machine was operated at 40 kV and the samples were analyzed between 2θ of 2^{o} to 80^{o} at a scan rate of 2^{o} per minute. The d values obtained from the

diffractograms were compared with standard JCPDS cards. In the present work, XRD have been used as an identification tool to confirm the presence of metal nanoparticles within the Pani matrix as zero valent metal **as** Pani exhibit d values at different 2θs.

2.3.4 Transmission electron microscopy (TEM) :

Principle

Transmission electron microscopy is an important technique that is being used extensively by the material research scientists as it actually reveals the shape and exact size as well as size distribution of the nanoparticles. Thus, XRD and TEM are complementary to each other but TEM is much more multifaceted in application as a single nanoparticle can be viewed or probed through TEM. Further, from the electron diffraction pattern, the hkl values of the planes can be easily measured and lattice planes can be predicted. In turn, the crystal structure can be evaluated more accurately.

The nanoparticle or nanocomposite samples in the present case were initially suspended in ethanol or methanol and sonicated for ~30 min. Then a drop or two of the sonicated samples were placed on a carbon coated copper grid of 400-mesh size. A JEOL, JEM 1200 instrument was used for the analysis. The instrument was operated at 200 kV and at 30 mA.

2.4 Sensor Fabrication and Measurements :

For carrying out sensor measurements, the synthesized nanocomposites were compressed into a pellet form (diameter 13 mm, thickness 3 mm) by applying a pressure of 7 tons using a Pye-Unicam die. The electrical contacts were made to the nanocomposite pellet with the help of copper wire and silver paste. Various types, as well as concentrations of analytes (methanol, ethanol, isopropanol, carbon tetrachloride, ammonia and chloroform) were prepared by using hexane as a diluent except for ammonia (diluent – double distilled water). The sensing performance of the nanocomposites were tested by subjecting the nanocomposite pellet to one of the analyte in a closed glass container at room temperature as shown in Fig.2.2 where the distance between the pellet and the analyte surface was kept approximately as 5 cm.

During sensing measurements, the change in the D.C. electrical resistance of the nanocomposite and blank polyaniline sensor was measured as a function of time for each concentration. The responses were recorded by exposing the sensor to the analyte vapours and air alternately after attaining equilibrium condition for each concentration of analyte for several cycles. The resistance was measured by using a two-probe method with a maximum measurement range up to 40 MΩ. The recorded results have been expressed as a plot of $\Delta R / R_0$ against time.

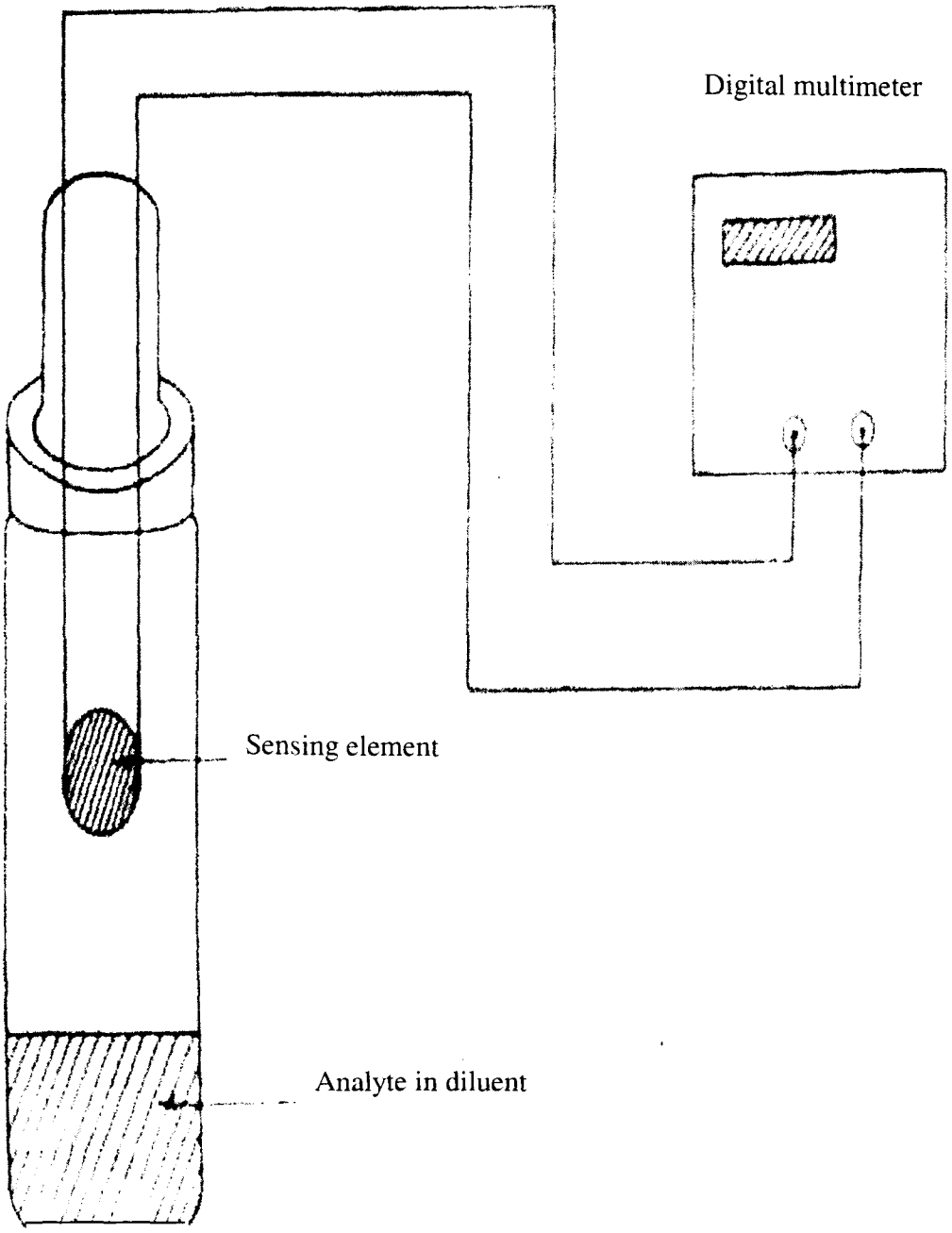

Fig. 2.2 Schematic representation of sensing measurement.